

Valency and spin states of substituent cations in $\text{Bi}_{2.15}\text{Sr}_{1.85}\text{CaCu}_2\text{O}_{8+\delta}$ T. M. Benseman,^{*} J. R. Cooper, C. L. Zentile, and L. Lemberger*Cavendish Laboratory, University of Cambridge, J. J. Thomson Avenue, Cambridge CB3 0HE, United Kingdom*

G. Balakrishnan

Department of Physics, University of Warwick, Coventry CV4 7AL, United Kingdom

(Received 5 December 2008; revised manuscript received 25 August 2011; published 4 October 2011)

We studied the valency and spin behavior of $M = \text{Mn, Fe, Co, Li, and Al}$ in the high-temperature superconducting compound $\text{Bi}_{2.15}\text{Sr}_{1.85}\text{Ca}(\text{Cu}_{1-z}\text{M}_z)_2\text{O}_{8+\delta}$ (Bi-2212) for small values of z . Mn, Fe, and Co retain their magnetic moments, and our thermopower and magnetic susceptibility data imply ionization states Mn^{3+} , Fe^{2+} , and Co^{2+} , while Li and Al are accommodated in the charge reservoir layers. Single-crystal studies show that the susceptibility of Co^{2+} ions in Bi-2212 is strongly anisotropic, with a weak anisotropy detected for Mn^{3+} and none for Fe^{2+} . Fits to a pseudogap formula for a pure Bi-2212 crystal suggest that the spin susceptibility of the host compound is more anisotropic than previously realized. Data in the superconducting state allow us to compare the pair-breaking properties of the different impurities. Several aspects of the data, including the stronger suppression of the superconducting transition temperature T_c by Co compared with Fe for underdoped and optimally doped samples, show that the d -level structure of the magnetic ions and multiorbital effects are important. We also find that the temperatures of the magnetization crossing points are equal to the low-field T_c values to within 1% or 2%. This agrees with a 2D thermodynamic fluctuation argument given by Junod *et al.*

DOI: [10.1103/PhysRevB.84.144503](https://doi.org/10.1103/PhysRevB.84.144503)

PACS number(s): 74.25.Ha, 74.62.Dh, 74.72.-h, 75.20.Hr

I. INTRODUCTION

Impurity substitution is a well-established technique for the study of high-temperature superconductors. In combination with microscopic probes, such as scanning tunneling spectroscopy (STS),^{1,2} angle-resolved photoemission spectroscopy (ARPES),³ and nuclear magnetic resonance (NMR),⁴ it is a powerful probe^{5,6} of the physics of high-temperature superconductivity (HTS). It is probable that impurity substitution will be used to build on recent advances, including the observation of (a) slow quantum oscillations from small pockets of electrons⁷ in single crystals of the yttrium barium copper oxide (YBCO) family in the underdoped, pseudogap (PG) region, (b) Fermi surface arcs in underdoped bismuth strontium copper oxide (Bi-2212) by ARPES,⁸ (c) local symmetry breaking from STS studies, namely, an orthorhombic distortion of the CuO_2 plaquettes in underdoped Bi-2212 crystals,¹ and (d) fast quantum oscillations corresponding to a large Fermi surface in overdoped superconducting crystals of the single-layer compound Tl-2201.⁹ It is now widely believed that some kind of broken symmetry is responsible for the PG and that this weakens the superconductivity. Our heat capacity¹⁰ and magnetic susceptibility¹¹ work shows that a nonzero PG sets in quite abruptly below a certain hole concentration (estimated to be $p \simeq 0.19$ holes/Cu), but there is no evidence for a sharp transition to the PG state as the temperature is reduced. Another key result of the heat capacity work is that in the PG region the electronic entropy is suppressed up to well above room temperature, which is difficult to reconcile with conventional spin or charge density wave order and tends to suggest a gradual crossover as the temperature is lowered. Impurities will have different effects on these unusual features depending on their valency and spin states, so it is helpful to determine these experimentally. From a practical viewpoint impurities are potentially important for pinning vortex lines and enhancing the current carrying capacity. Rather low concentrations may

be effective because when 1% of the Cu sites are substituted, the vortex lattice spacing only becomes equal to the distance between impurities in any given CuO_2 plane at extremely large magnetic fields ~ 300 T.

Here we substitute a small fraction of the Cu atoms in the HTS compound $\text{Bi}_{2.15}\text{Sr}_{1.85}\text{CaCu}_2\text{O}_{8+\delta}$ (Bi-2212) with the transition metals Mn, Fe, and Co. We show that these all retain their magnetic moment, and we have also investigated Al and Li as nonmagnetic substituents. Although Zn substitution has been used to study YBCO^{11,12} and lanthanum strontium copper oxide (LSCO),^{13,14} it has a very low solubility limit in Bi-2212 (at most 1% of the Cu atoms¹⁵), making it less suitable here.

This paper is organized as follows: Sec. II gives details of the preparation of the substituted polycrystalline and single-crystal samples, and Sec. III deals with the superconducting transition temperatures T_c and the solubility limits of the various elements studied. Sections IV and V are devoted to our measurements and discussion of the thermoelectric power (TEP), or $S(T)$, and lattice parameters respectively. Section VI A deals with magnetic measurements of both polycrystalline and single crystals above T_c and their analysis, which allows us to determine the magnetic moments of Mn, Fe, and Co and compare with valencies from the TEP results in Sec. IV. Section VI B summarizes magnetic data below T_c from which we obtain the magnitude and T dependence of the London penetration depth. The main conclusions are given in Sec. VII.

II. SAMPLE PREPARATION

We prepared polycrystalline sintered samples with nominal stoichiometry of $\text{Bi}_{2.15}\text{Sr}_{1.85}\text{Ca}(\text{Cu}_{1-z}\text{M}_z)_2\text{O}_{8+\delta}$, with $M = \text{Mn, Fe, Co, Li, or Al}$, at various levels of impurity substitution.¹⁶ Appropriate weights of the dried starting materials, Bi_2O_3 , SrCO_3 , CaCO_3 , and CuO (plus Co_3O_4 ,

Fe_3O_4 , Li_2CO_3 , or Al_2O_3), were ground under cyclohexane in an agate mortar and pestle and heated in Al_2O_3 crucibles in flowing zero-grade air at temperatures up to 820°C until weight loss showed that most of the CO_2 had been lost. They were then reground, pressed into pellets, placed on gold foil in an Al_2O_3 crucible, and heated in flowing air at temperatures up to 865°C . This process was repeated up to nine times, until impurity phases could no longer be detected by powder x-ray diffraction. Generally four to six samples with different values of z were prepared simultaneously.

We have also grown single crystals by the traveling solvent floating zone method (TSFZ) in Warwick using a Crystal Systems Incorporated 4-mirror image furnace, with $M = \text{Fe}$, Co , and Li and $z = 0.02$, using approximately 40 g of phase-pure polycrystalline starting material. We found that Mn has a lower solubility limit, and so single crystals of Mn were grown with $z = 0.01$. Al has an even a lower solubility limit (as will be shown below) and so was not used for single-crystal growth.

III. T_c AND SOLUBILITY LIMITS

In the cuprates, T_c is strongly influenced by the hole concentration p and can be described by the empirical function

$$T_c = T_c^{\max}[1 - 82.6(p - 0.16)^2], \quad (1)$$

where p is the number of holes per Cu atom and T_c^{\max} is the maximum T_c for the compound.¹⁷ Our unsubstituted polycrystalline and single-crystal samples both have $T_c^{\max} = 86.5\text{ K}$. Substituting the Cu site is expected to reduce T_c^{\max} because a d -wave superconductor is strongly affected by any impurities, which increase the scattering rate, while substitution of the Cu or other sites with altermvalent impurities changes p . As the mobile charge carriers in Bi-2212 are largely confined to the CuO_2 planes, an impurity potential at a planar Cu site is expected to scatter the carriers far more strongly, and depress T_c by a greater amount, than one located on a cation site in a reservoir layer. Figure 1 shows T_c as a function of substitution level for the polycrystalline bars studied in this experiment. To ensure oxygen homogeneity, these were annealed at 400°C in flowing N5.0 grade O_2 for 48 h and then quenched into liquid nitrogen so they are all slightly overdoped. T_c was then measured by ac susceptometry (ACS) using a rms field of 1 G at 333 Hz.¹⁸ The strong depression of T_c at high levels of cobalt substitution suggests that Co has the highest solubility limit of the cations investigated, followed by Fe, in agreement with the findings of Maeda *et al.*¹⁹ and Kluge *et al.*¹⁵ for polycrystalline samples, as well as studies of Bi-2212 whiskers by Kuo *et al.*²⁰ but this is discussed again later. Mn and Al show no depression in T_c above 1% substitution, while Li continues to reduce T_c slowly up to the 10% level. The TEP data show that this is mainly caused by a small increase in hole doping with Li substitution. By comparison in optimally doped $\text{YBa}_2\text{Cu}_3\text{O}_{7-\delta}$, T_c is depressed by around 5 K/% Li ,²¹ and the ^7Li NMR shift has a Curie-like T dependence with the Weiss θ increasing from small values in the PG region to large ones on the overdoped side.^{4,21}

Figure 2 shows the effect of these impurities on the melting point of Bi-2212, as measured by differential thermal analysis (DTA) using a Stanton Redcroft 1500 analyzer. An impurity

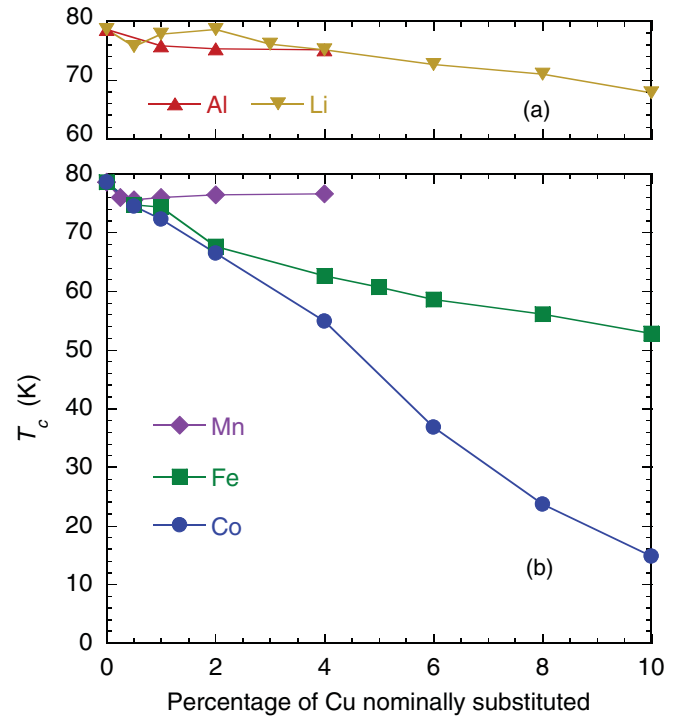


FIG. 1. (Color online) T_c plotted as a function of nominal substitution level for the five substituent cations investigated in this work. Errors in T_c are equal to the size of the symbols used.

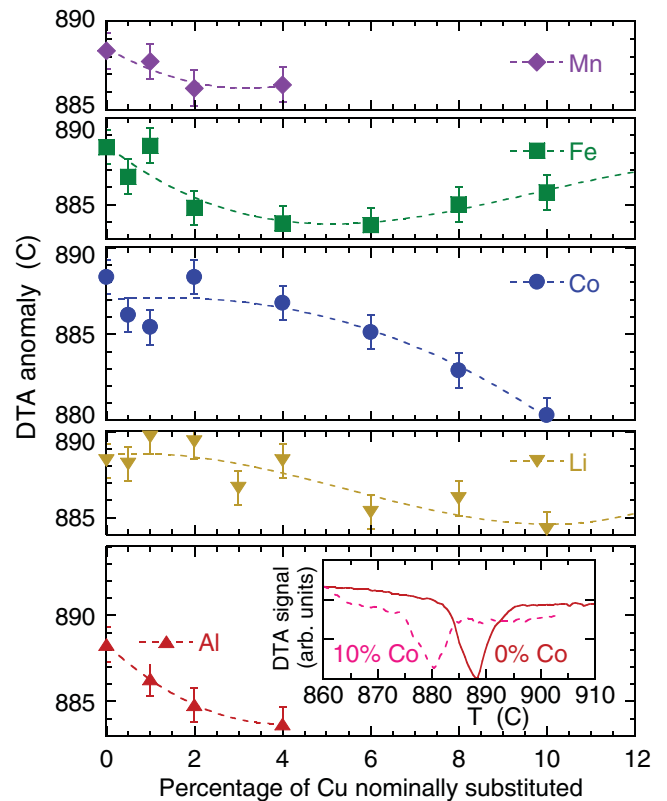


FIG. 2. (Color online) Melting temperature as measured by differential thermal analysis performed in flowing air, warming at $2^\circ\text{C}/\text{min}$. Dotted lines are polynomial fits to measured points. The inset shows the width of typical melting anomalies

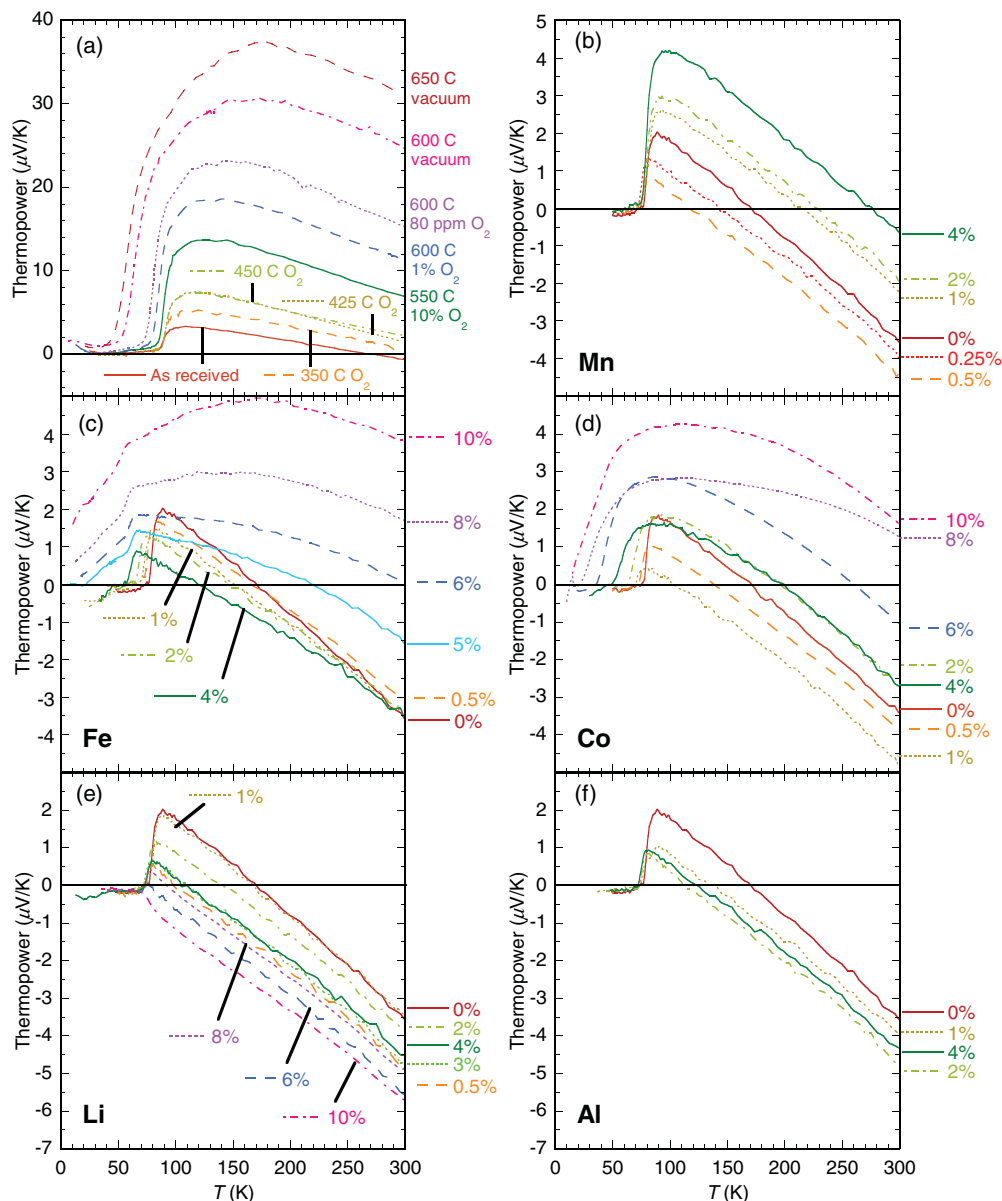


FIG. 3. (Color online) (a) $S(T)$ for 15% Y-substituted sintered Bi-2212 bars for a range of annealing conditions. (b)–(f) $S(T)$ for overdoped sintered bars annealed in flowing O_2 at 400°C. For the 5%–10% Fe-doped samples in (c), T_c measured by ACS corresponds to the sharp knee in $S(T)$. Nonzero values of $S(T)$ below T_c are ascribed to poor intergranular coupling.

in solid solution is expected to lower the melting point, but this may depend on the substitution site. The plot suggests a solubility limit in excess of 10% for Co and Li, 3% for Al, 2% for Mn, and, as discussed later, possibly around 4% for Fe. However, the limits for substitution on the Cu site are generally lower.

IV. THERMOPOWER

The valency of a substituent is important because the physical properties of HTS compounds depend strongly upon the carrier concentration p . Replacing Cu^{2+} with a trivalent cation will dope an electron into the compound (assuming that the oxygen concentration is unchanged), reducing p , while substituting it with a monovalent ion will add an extra

hole. The room-temperature thermopower $S(290\text{ K})$ of the HTS cuprates (with the exception of the LSCO compounds) shows a quasiuniversal behavior with respect to p ,²² expressed numerically as²³

$$S(290\text{ K}) = \begin{cases} -139p + 24.2 & (p \geq 0.155), \\ 992 \exp(-38.1p) & (0.05 < p < 0.155), \end{cases} \quad (2)$$

where $S(290\text{ K})$ is given in $\mu\text{V/K}$ and p is given in holes per Cu atom. In principle this can be used to separate the effects of disorder and changes in p on T_c .²⁴ However, although we assume throughout this paper that Eq. (2) applies to all our data, some caution must be applied, especially for Co- and Fe-doped samples with $z \geq 0.04$, where, as shown in Fig. 3, $S(T)$ shows unusual curvature for low values of p .

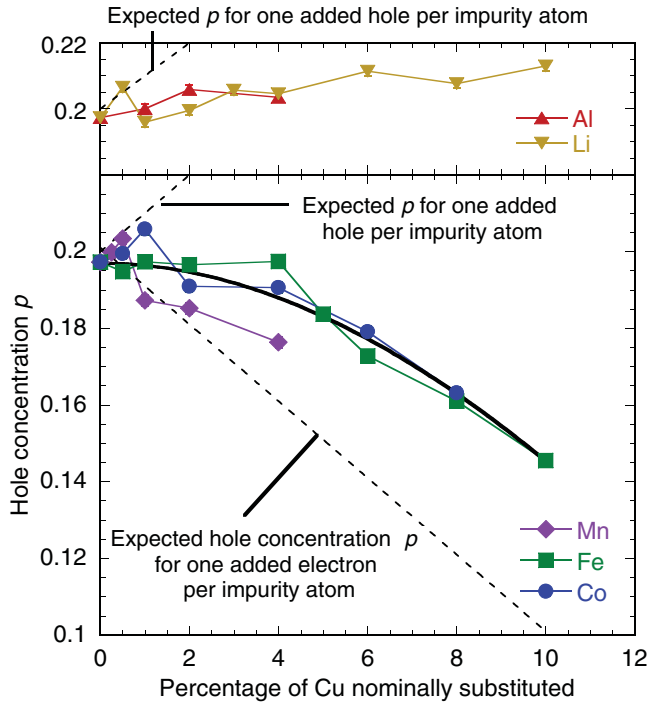


FIG. 4. (Color online) Hole concentration p as calculated from $S(290\text{ K})$ using Eq. (2) for overdoped sintered Bi-2212 bars. Errors in p are approximately the size of the symbols used. The solid line shows the behavior expected for random distribution of ions on Cu sites where every Fe or Co ion with at least one Fe or Co near neighbor has a mean valency of 3.5+, while isolated ions have a valency of 2+.

Li and Al are expected to form Li^+ and Al^{3+} ions in Bi-2212, whereas for the transition-metal substituents, the oxidation state is difficult to predict. Electron counting of the type described above will only work if the oxygen content is unaltered, so that the thermoelectric power is a useful practical guide to the changes in p caused by the various impurities. $S(T)$ data are shown for pure and substituted Bi-2212 in Fig. 3, while p values determined from $S(290\text{ K})$ and Eq. (2) for all impurity species investigated here are plotted in Fig. 4. In Fig. 3(a) we also plot $S(T)$ for 15% Y-substituted Bi-2212 to show the effect of underdoping by oxygen depletion. Samples from the same batch were also used for heat-capacity measurements by Loram *et al.*¹⁰ We notice from Fig. 4 that Fe substitution has no apparent effect on the hole concentration up to $z = 0.04$, suggesting it has state Fe^{2+} . Within the scatter of the data Co shows the same behavior.

In Fig. 5(a) we show $S(290\text{ K})$ versus T_c . At first sight the points for Fe doping suggest that Fe goes on a different site for $z > 4\%$ and starts to reduce p there. However, there is an unexpected result in Fig. 5(b): for $z = 0.04$, Co causes a factor of 2 larger depression of T_c than Fe for $p \leq 0.16$, but there is only a 20% difference for $p \simeq 0.2$. Because the p values for Co and Fe samples in Fig. 4 are similar for all z , we believe the differences between Fe and Co shown in Figs. 1 and 5(a) are mostly caused by the different suppression of T_c for $p \leq 0.19$ shown in Fig. 5(b). From this viewpoint the changes in p above $z = 0.04$ for both Fe and Co either arise

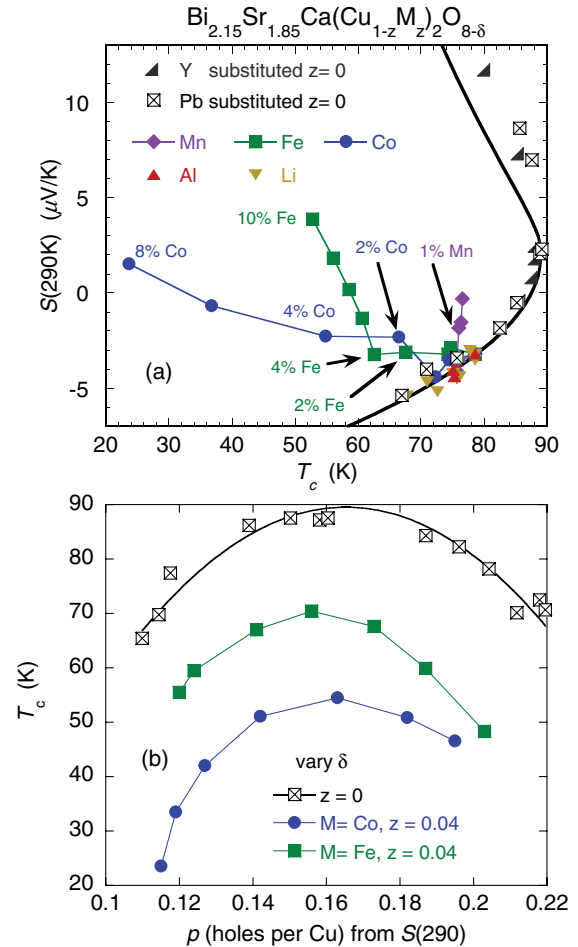


FIG. 5. (Color online) (a) Room-temperature thermopower $S(290\text{ K})$ vs T_c . All the substituted samples were annealed at 400°C in 100% O_2 . The solid line corresponds to Eq. (1) with $T_c^{\text{max}} = 89\text{ K}$ and Eq. (2). (b) Variation of T_c (determined from ACS and the TEP) vs hole concentration per planar Cu p , determined from $S(290\text{ K})$ using Eq. (2). This shows that Fe substitution gives a smaller depression of T_c than Co for underdoped and optimally doped samples. The oxygen deficiency δ was altered by annealing at various temperatures and quenching into liquid nitrogen. Fe- and Co-doped samples with similar values of p were annealed together. Data for $z = 0$ are taken from Ref. 25. The solid line through the $z = 0$ points corresponds to Eq. (1) with $T_c^{\text{max}} = 89\text{ K}$ and $p_{\text{opt}} = 0.165$.

from substitutions on other sites or because near-neighbor pairs have a larger valency, which would produce the solid line in Fig. 4. Alternatively, these changes in p might be caused by changes in electron transfer from the reservoir layers as the electronegativity of the CuO_2 planes is altered by Co or Fe substitution.

From Fig. 4 we see that for $z \leq 0.01$ every Mn ion adds one hole, i.e., the valency of Mn is 3+ when it substitutes for Cu. The data for Mn in Fig. 5(a) suggest that only 0.5%–1% substitute for Cu and that for a fixed value of $S(290\text{ K})$, i.e., p , Mn gives a similar initial slope $dT_c/dz = -6\text{ K}/\%$ as Co and Fe. Within experimental error the data for Li and Al in Fig. 5(a) lie on the same curve as the data for O-deficient samples with non-pair-breaking impurities, such as Y and Pb. This suggests that, at most, a very small fraction of the Al or Li atoms

replace Cu, and their main effect is to give small changes in p . This is consistent with their extremely weak effect on $\lambda_{ab}(T)$, shown later [Figs. 9(d) and 9(e)]. Finally, to conclude this section we also note in Fig. 4 the small “knee” in p [derived from $S(290\text{ K})$] versus z occurring at around 1% substitution for Mn and Co. As discussed below this could arise from the incorporation of extra oxygen for $z \simeq 0.01$. Intriguingly, the effect of this knee is to bring the anomalous points on to the “non-pair-breaking” line in Fig. 5(a).

V. X-RAY DIFFRACTION

As mentioned earlier, the powder x-ray diffraction spectra of all samples were single phase with the exception of Fe-doped samples with $z \geq 0.05$. Replacing a Cu atom with a cation of different atomic radius is expected to change the lattice parameters (a , b , and c) of the crystal. To measure this, sintered bars were once again annealed in 100% N5.0 grade O_2 at 400°C for 48 h and quenched into liquid nitrogen. They were then ground into powder and mixed with a powdered Si standard. X-ray diffraction spectra were collected at 298 K using a Siemens Kristalloflex powder diffractometer and Cu $K\alpha$ radiation. When fitting diffraction patterns, we assume that $a = b$ since for Bi-2212 a and b are too similar for the relevant lines to be distinguished. Results are plotted in Fig. 6. We see a small decrease in a (less clearly in c) with increasing Li and Al substitution. This might be expected on replacing Cu^{2+} with Li^+ or Al^{3+} ; however, our T_c and thermopower data suggest that only a small fraction of the Li or Al ions actually substitute on the Cu site. Mn and Co show a systematic decrease in c , as does Fe up to the 6% level. The increase in c for higher levels of Fe substitution may be due to Fe ions assuming a different valency and are consistent with them locating upon a different site. Finally, we observe anomalies in the lattice parameters (especially a) at low substitution levels for Mn (around 1%), Co (1%), and Li (0.5%). The substitution levels at which these occur closely agree with similar anomalies in $S(290\text{ K})$ versus p (as plotted in Fig. 4), suggesting that they may both be due to small concentrations of substituents, at the 1% level, increasing the O content by 0.02 oxygen atoms per formula unit. Babaei pour and Ross²⁶ report an initial decrease in a of 0.16 \AA per added oxygen in pure Bi-2212. So within this picture 1% Co would give a change of -0.0032 \AA in a , comparable to the anomalous initial changes in Fig. 6. It would also be expected to increase p by about 0.02, larger but of the same order as the anomalies seen in $S(290\text{ K})$.

VI. DC SUSCEPTIBILITY

A. Normal state

Results of magnetic susceptibility measurements for polycrystalline samples are shown in Fig. 7. Corresponding single crystal data, which provide estimates of the magnetic anisotropy, are shown in Fig. 8. For pure Bi-2212, we fit the normal-state susceptibility to the model proposed by Loram *et al.*¹⁰ for the electronic contribution to the specific heat and magnetic susceptibility of the cuprates. In this model, the

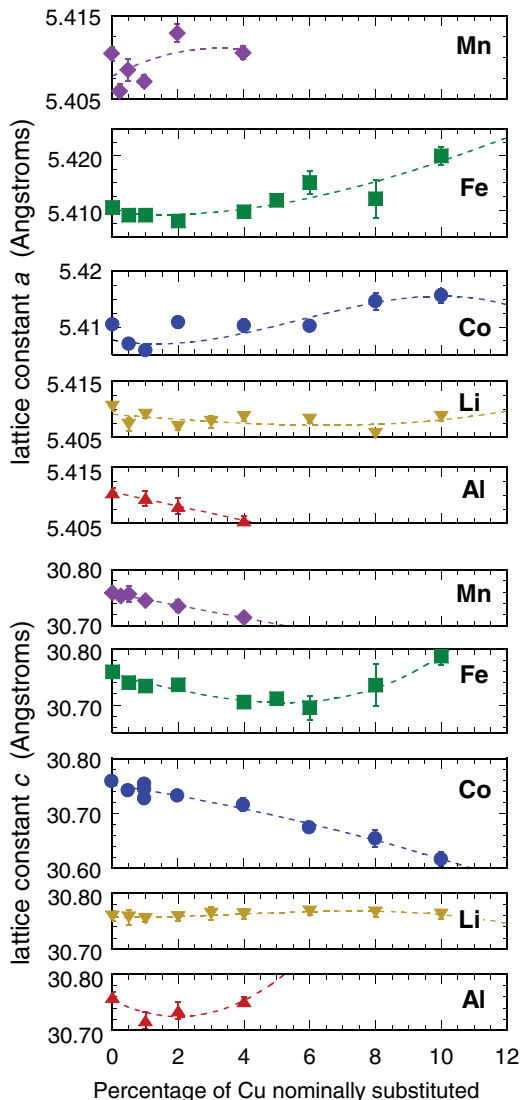


FIG. 6. (Color online) Lattice parameters measured via Cu $K\alpha$ x-ray powder diffraction on overdoped Bi-2212. Dashed lines are polynomial fits to measured points.

density of states in the normal state has a triangular “notch” centered at the Fermi energy ϵ_F for $p < 0.19$, namely,

$$N(E) = \begin{cases} N_0 \frac{|E|}{E_g} & (|E| \leq E_g), \\ N_0 & (|E| > E_g), \end{cases} \quad (3)$$

where E is measured from ϵ_F , E_g is the pseudogap energy, and N_0 is a constant, independent of p and E . The magnetic spin susceptibility χ_s is given by

$$\chi_s = 2\mu_B^2 \int_0^\infty N(E) \left(-\frac{\partial f}{\partial E} \right) dE \quad (4)$$

$$= \frac{\mu_B^2}{2k_B T} \int_0^\infty N(E) \cosh^{-2} \left(\frac{E}{2k_B T} \right) dE, \quad (5)$$

where f is the Fermi-Dirac function.

Substituting Eq. (3) into Eq. (5) yields the following expression for the temperature-dependent susceptibility:²⁷

$$\chi_s(T) = N_0 \mu_B^2 \left\{ 1 - \left(\frac{E_g}{2k_B T} \right)^{-1} \ln \left[\cosh \left(\frac{E_g}{2k_B T} \right) \right] \right\}. \quad (6)$$

For $p \geq 0.19$ we take $E_g = 0$ and model the susceptibility of pure Bi-2212 with a Kondo-like T dependence of the form

$$\chi(T) = \frac{C_{\text{pure}}}{T + 110} + A, \quad (7)$$

where the main part of $\chi(T)$ is a constant (A). For the pure sample with $p = 0.197$, we find that $A = 1.1 \times 10^{-4}$ emu/mole and $C_{\text{pure}} = 2.0 \times 10^{-3}$ emu K/mole. For impurity-doped samples we subtract the contribution from the pure sample annealed under the same conditions from $\chi_{\text{total}}(T)$ and fit the remaining susceptibility to a Kondo-like temperature dependence:

$$\chi_{\text{impurity}}(T) = \frac{C}{T + \theta}. \quad (8)$$

Results of fits to polycrystalline samples are shown in Figs. 7(b) and 7(c). In the case of Co these should be interpreted with caution, since for Co, $\chi_{H \parallel c}$ and $\chi_{H \perp c}$ have significantly different C and θ values, as can be seen from Fig. 8(g).

Single crystals used for SQUID measurements were cut to approximately $4 \times 4 \times 0.5$ mm³ $a \times b \times c$ (typical sample weights were around 50 mg) using a fine-wire saw and then annealed at 600 °C in N5.0 grade O₂ followed by quenching on to a copper block to ensure oxygen homogeneity. This higher temperature was used for equilibrating single crystals since equilibration of a single crystal of these dimensions at 400 °C as was done for polycrystalline samples would require several months.²⁸ We find the susceptibility of pure Bi-2212 single crystals to be surprisingly anisotropic, agreeing closely with results reported for this doping level ($p = 0.175$) by Watanabe *et al.*²⁹ We make the reasonable assumption that E_g represents a gap in the quasiparticle excitation spectrum and cannot depend on the orientation of H . Then the data for pure Bi-2212 shown in Fig. 8(a) can only be fitted to Eq. (6) if there is larger anisotropy in the spin susceptibility [$\chi_s(H \parallel c) / \chi_s(H \parallel ab) = 1.5 \pm 0.1$] than previously thought. We have reached a similar conclusion recently from magnetic anisotropy measurements on YBa₂Cu₄O₈.³⁰

For a molar concentration $2z$ of a magnetic impurity in which the total orbital angular momentum of the electrons (L) is fully quenched, i.e., $\langle L^2 \rangle \neq 0$, $\langle L_x \rangle = \langle L_y \rangle = \langle L_z \rangle = 0$ (as we would expect in the case of a transition-metal ion located on the Cu site in Bi-2212, which has half-octahedral symmetry and presumably a strong crystal field), the susceptibility per mole Bi-2212 is

$$\chi = \frac{2z N_A g^2 S(S+1) \mu_B^2}{3k_B (T + \theta)} \quad (9)$$

$$= \frac{2z N_A p_{\text{eff}}^2 \mu_B^2}{3k_B (T + \theta)}, \quad (10)$$

where p_{eff} is the effective number of Bohr magnetons.³¹ By fitting our single-crystal data to Eq. (8), we obtain p_{eff} from Eq. (10) and can thereby infer the oxidation state. We

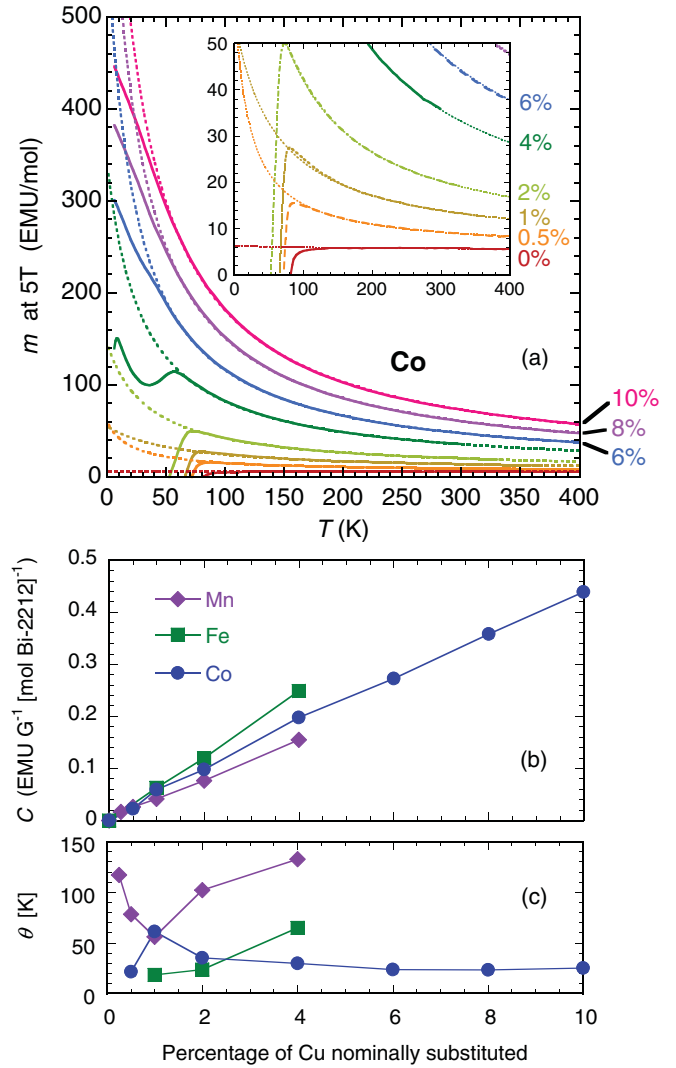


FIG. 7. (Color online) (a) Molar magnetic moments of Co-substituted polycrystalline samples annealed and quenched as for those shown in Figs. 1 and 4, measured at 5 T. Fits to the normal-state data are shown as dotted lines, being of the form $m = (\chi_{\text{Bi-2212}} + \chi_{\text{impurity}})H$ (in CGS units). (b) and (c) Magnitude of Curie constant C and Kondo temperature θ , respectively, from fits to Eq. (8) in (a), plotted together with equivalent data for Mn and Fe.

assume nominal concentrations ($2z$) when calculating χ for our samples. For the single-crystal samples substituted with transition metals, we have confirmed these concentrations by electron-probe microanalysis (EPMA). By contrast, for a sintered polycrystalline sample that has not been melted at any stage of its preparation, segregation of impurity phases would not be expected to occur over a length scale greater than the grain size. For polycrystalline Bi-2212 prepared here the mean grain size was only 250 nm,³² so any impurity segregation would not be detected to within the 1- μ m spatial resolution of EPMA.

In an attempt to study the energy levels of the orbitals of the various impurities investigated here, 10-GHz electron-spin-resonance (ESR) measurements were performed upon single crystals. No ESR signals could be detected for any of the

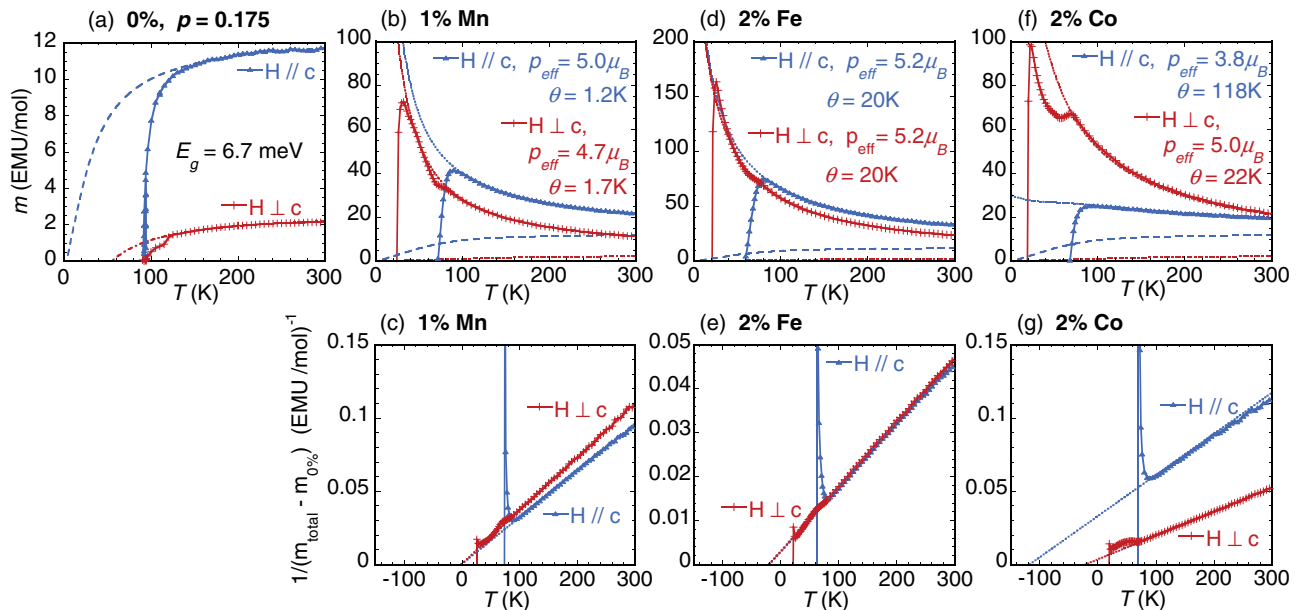


FIG. 8. (Color online) Molar magnetic moments measured at 5 T for single crystals investigated in this work. (a) Curves for a slightly overdoped, unsubstituted sample, showing normal-state and superconducting diamagnetic transition. The dashed lines are fits of Eq. (6) to the normal state, including a T -independent isotropic contribution to χ of -1×10^{-4} emu/mole arising from nonspin contributions such as the core diamagnetism. These curves were subtracted before fitting the data for the impurity-substituted crystals to Eq. (8). (b), (d), and (f) Data for the single crystals doped with magnetic impurities, with fits for $m_{\text{total}} = m_{\text{Bi-2212}} + m_{\text{impurity}}$ shown as dotted lines and the pure Bi-2212 contribution shown as dashed lines. (c), (e), and (g) The inverse of the impurity contribution to the moments, which clearly fit a Curie-Weiss law [Eq. (8)] with θ values given by the negative intercept. χ_{Co} is strongly anisotropic, χ_{Mn} is slightly so, and χ_{Fe} is isotropic within experimental error.

samples. This is consistent with our other results since in a metallic environment a relatively narrow ESR line is only expected to exist for a half-filled d shell. This implies that there are no impurity ions present in our samples with half-filled d shells, i.e., no Mn^{2+} , Fe^{3+} , or Co^{4+} .

B. Superconducting state

To investigate the effects of cation substitution on the superconducting magnetization properties, field-cooled dc-SQUID temperature sweeps were performed on warming at 0.5, 1, 2, 3, 4, and 5 T from 6 K up to a few Kelvin above T_c . The fits to the normal-state susceptibility described in Sec. VIA were then subtracted from these data.

Hao and Clem³³ derive the following expression for the reversible magnetization of a type II superconductor (with Ginzburg-Landau parameter $\kappa \gg 1$) with field penetration depth λ :

$$-4\pi M = \alpha \left(\frac{\phi_0}{8\pi\lambda^2} \right) \ln \left(\frac{\beta H_{c2}}{H} \right). \quad (11)$$

In the standard London model, the constants α and β are assumed to be equal to 1, but refinements to the model are necessary when the effects of the vortex cores on the free energy are taken into account.³³ This results in refined estimates for α and β , which depend slightly upon the value of H/H_{c2} . For the fields under which we study the magnetization of our samples and with typical estimates of $H_{c2} \approx 100$ T for Bi-2212, we obtain $\alpha = 0.77$ and $\beta = 1.44$, and these values will be used for the analysis performed below.

For a polycrystalline superconducting sample showing high anisotropy ($\lambda_c^2 \gg \lambda_{ab}^2$) the magnetization is dominated by currents flowing in the ab plane. If the anisotropy in λ is sufficiently large (in practice, if $\gamma = \lambda_c^2/\lambda_{ab}^2 \geq 5$, using the notation of Triscone *et al.*³⁴), then the magnetization will be nearly independent of λ_c . Employing the appropriate angular averaging, Triscone *et al.*³⁴ calculate the magnetization for such a sample to be given by

$$-4\pi M = \alpha I(\gamma)/\gamma \left(\frac{\phi_0}{8\pi\lambda_{ab}^2} \right) \ln \left(\frac{\beta e(\gamma) H_{c2}(H\parallel c)}{H} \right) \quad (12)$$

where the functions $I(\gamma)/\gamma \rightarrow 0.51$ and $e(\gamma) \rightarrow 1.66$ in the anisotropic limit (i.e., as $\gamma \rightarrow \infty$).³⁴ We calculate M from the sample moment by taking the volume of the sample to be $V = m_s/\rho_{\text{Bi-2212}}$, where m_s is the sample mass and $\rho_{\text{Bi-2212}} = 6.69\text{g/cm}^3$ is obtained from the lattice parameters. We also assume that for $H \geq 0.5$ T, the observed magnetization will not be influenced by intergrain currents. Since the sample moment has been measured at six values of H at each temperature studied, after correcting for the extrapolated normal-state contribution [i.e., $M = \chi_{\text{fit}}H$, where $\chi_{\text{fit}} = \chi_{\text{Bi-2212}}(T) + \chi_{\text{impurity}}(T)$], we may fit the data to

$$M = a_0 + a_1 \ln(H) \quad (13)$$

and hence determine $\lambda_{ab}^2(T)$ and $H_{c2}(T)$. $1/\lambda_{ab}^2(T)$ is of particular interest to us, being proportional to the superfluid density. When an impurity species is soluble in Bi-2212 and goes on the Cu site, we expect the resulting scattering to reduce the effective superfluid density.

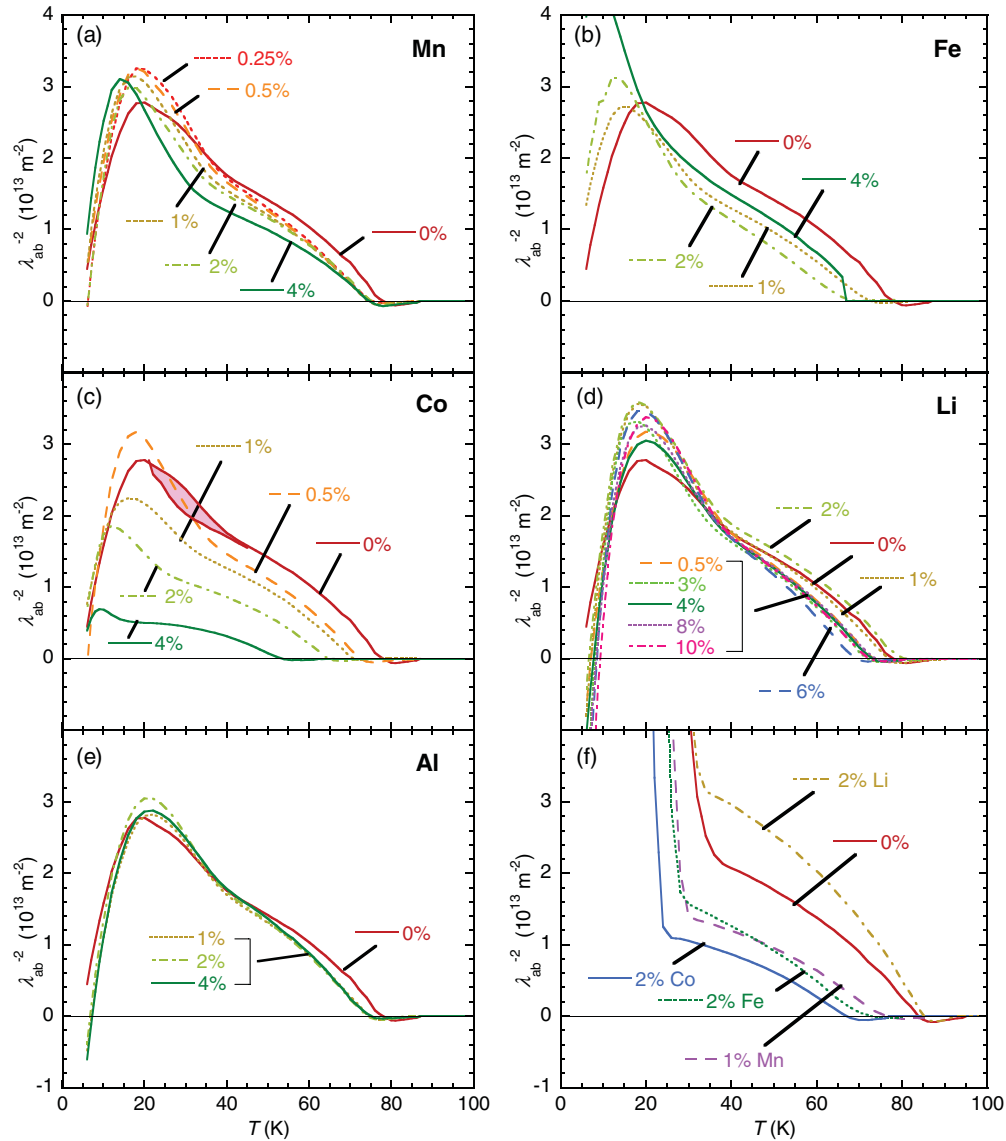


FIG. 9. (Color online) Estimates of $1/\lambda_{ab}^2(T)$ derived from $M(H, T)$ and Eq. (13). (a)–(e) show data for polycrystalline samples, annealed in 100% O_2 at $400^\circ C$ (giving $p = 0.194$ for pure Bi-2212). (f) shows curves for the less heavily overdoped single crystals annealed in 100% O_2 at $600^\circ C$ ($p = 0.175$ for pure Bi-2212) whose normal-state susceptibility was plotted in Fig. 8, measured with $H \parallel c$.

Taking into account thermal fluctuations of the positions of vortices (which are far more significant in a nearly two-dimensional superconductor), Bulaevskii *et al.* predict an additional feature in $M(H, T)$: at a temperature T^{cr} , which depends on the interlayer lattice spacing and on κ , $M(H, T^{cr})$ should be independent of H , resulting in a point at which measured curves for $M(T)$, when corrected for χ_{NS} , converge and cross each other.³⁵ Triscone *et al.* have experimentally verified the existence of such a crossing point for several HTS compounds, typically a few Kelvin below T_c .³⁴ However, from a different, critical fluctuation viewpoint, Junod *et al.*³⁶ have argued that the crossing point is actually T_c . We observe a crossing point in our results, indicating that our fitted normal-state susceptibilities are adequate, at least near this crossover region. We define T^{cr} as the temperature at which the regression coefficient a_1 in Eq. (13) crosses zero. When the normal-state susceptibility is large (e.g., for

samples heavily substituted with magnetic ions), determining T^{cr} is more difficult. For all single crystals studied, T^{cr} with $H \parallel c$ is within $\pm 1\%$ of T_c determined by low-field ACS. For the polycrystalline bars T^{cr} is generally within $\pm 2\%$ of T_c . We therefore think that this observation favors the critical fluctuation viewpoint of Junod *et al.*

We have used Eqs. (12) and (13) to obtain values of $\lambda_{ab}^2(T)$ shown in Fig. 9. Depending on the sample, the data give reliable values of $\lambda_{ab}^2(T)$ above 20–40 K where the sample is in the reversible region. We observe a significant depression of the effective superfluid density with Fe and Co substitution. Co has a larger effect for concentrations ≤ 4 at. %, where both impurities are thought to substitute the Cu site. We suspect this interesting difference is connected in some way to the different effects of Fe and Co on T_c shown in Fig. 5(b). No appreciable superfluid density could be detected in the $M(H, T)$ curves at substitution levels of 6% and above.

TABLE I. Summary of findings for impurity magnetic moments in this work compared with moments for possible ionization states taken from Kittel.³¹ The predicted values assume that the orbital angular momenta are fully quenched due to crystal field effects. The most likely dilute limit ionization state for each impurity, in light of our thermopower and single-crystal susceptibility results, is shown in boldface.

Ion	Configuration	Basic level	$p_{\text{eff}} = 2[S(S+1)]^{1/2}$	p_{eff} observed $H \parallel c$	p_{eff} observed $H \perp c$
Mn³⁺	3d⁴	⁵D₀	4.90	5.0 ± 0.1	4.7 ± 0.1
Mn ²⁺	3d ⁵	⁶ S _{5/2}	5.92		
Fe ³⁺	3d ⁵	⁶ S _{5/2}	5.92		
Fe²⁺	3d⁶	⁵D₄	4.90	5.2 ± 0.1	5.2 ± 0.1
Co ³⁺	3d ⁶	⁵ D ₄	4.90		
Co²⁺	3d⁷	⁴F_{9/2}	3.87	3.8 ± 0.1	5.0 ± 0.1

For Mn the effect is weaker. Although our results for T_c suggest that Mn is less likely to substitute for Cu in Bi-2212 than Co or Fe, the thermopower data in Figs. 1(b) and 4(b) show that Mn has a tendency to reduce p . This is supported by the valency 3+ obtained from the magnetic moment shown in Table I. Hence for the polycrystalline samples that have $p = 0.19$ the effect of Mn on λ_{ab} is weaker because of a cancellation of pair-breaking effects and the increase in T_c caused by lowering p . But from the single-crystal data with $p \simeq 0.175$ in Fig. 9(f) it can be seen that 1% Mn gives comparable pair-breaking effects to 2% Co and slightly more than 2% Fe.

For Al substitution $\lambda_{ab}^{-2}(T)$ is almost unchanged above the 1% level. Li substitution of 3% or more gives a small reduction of superfluid density, but this effect shows no systematic trend and is weaker than that seen for Fe or Co. The changes in λ_{ab} for Al and Li are therefore entirely consistent with the conclusions reached before from the thermopower results in Figs. 1(b) and 4(b), i.e., only a small fraction of the Al or Li atoms substitute on the Cu site; hence there is little pair breaking. On the other hand, 2% Li substitution in a single crystal with $p = 0.175$ appears to *increase* the superfluid density, which is another interesting and unexplained result.

The increase in the slope of the curves below around 40 K in Figs. 9(a)–9(d) and the downturn below around 20 K correspond to the samples entering the irreversible region, whereupon the superfluid density can no longer be determined in the above manner. Furthermore, when any of the temperature sweeps at lower fields are in the irreversible region, the fit to $\ln(H)$ will be affected. We believe that the apparent change in $\partial\lambda_{ab}^{-2}/\partial T$ (occurring below 40 K for the unsubstituted sample) may be an artifact of this. This is supported by the data for 0% Co shown in Fig. 9(c), where the shaded region indicates how estimates of λ_{ab}^{-2} change when lower fields are omitted from the fit. The lower boundary of this region is obtained using $M(4\text{ T})$ and $M(5\text{ T})$ only.

VII. CONCLUSIONS

Table I shows a summary of our susceptibility results. We have also investigated hole-doping levels as low as $p = 0.14$ and have found only minor shifts in the impurity moments, relative to those shown here. Likewise, the strongly anisotropic behavior of Co is not significantly affected by changes in hole doping. With regard to valency the clearest result is that for Fe, where the spin per impurity ion and the lack of an apparent

effect upon the thermopower imply that it is Fe²⁺ in Bi-2212 at substitution levels up to 4% of the Cu sites. This means that Fe is of particular interest for study as a magnetic impurity in Bi-2212 since in low concentrations it has no significant effect upon the carrier concentration. But this simple picture breaks down for higher Fe (and probably also Co) contents, either because additional Fe dopants go to another lattice site or (less likely) because ions in nearest-neighbor pairs have a higher valency. The thermopower results in Fig. 1(b) point toward Co having state Co²⁺ for $z \leq 0.04$, but for $z \leq 0.01$ there are anomalies in plots of $S(290\text{ K})$ and a -axis lattice parameter versus z that could be caused by the uptake of extra oxygen atoms. The large susceptibility anisotropy and the very high Curie-Weiss temperature for Co with $H \parallel c$ are matters for further investigation. For comparison, note that for Co-doped polycrystalline YBCO, the spin per impurity atom is $3.7 \pm 0.2\mu_B$,³⁷ although we are not aware of any measurements of the anisotropy in χ . For Co it is unclear whether the observed Curie-Weiss θ represents a true Kondo effect or a crystal field effect. For Fe and Mn, which are essentially isotropic, the θ values are reasonably constant for $z \leq 0.02$, with average values of 21 ± 3 and 88 ± 27 K, respectively, suggesting that they could be single-impurity Kondo temperatures.

In summary we find that up to 10 at. % Li can be incorporated into Bi-2212, reducing T_c by $\simeq -2\text{K/at. \%}$. However, our thermoelectric power and penetration depth data strongly suggest that the suppression of T_c arises from a small increase in p and not from pair breaking. Surprisingly, trivalent Al also has a very small effect. In other words, despite being nominally substituted for Cu these two nonmagnetic impurities seem to be mainly located outside the CuO₂ planes in Bi-2212, although rather strangely Al does reduce the in-plane lattice parameter. Our TEP and magnetic susceptibility measurements show that the valency of the three magnetic ions in critically doped ($p \simeq 0.19$) Bi-2212 are Fe²⁺, Co²⁺, and Mn³⁺. Of these, Co shows considerable magnetic anisotropy, which is perhaps surprising in a metallic environment, while Fe and Mn are essentially isotropic. Although all three magnetic ions give similar initial suppression of the superconducting transition temperature, $T_c \simeq -6\text{ K/at. \%}$, when $p \simeq 0.19$, as shown in Fig. 1(b) Co gives a larger suppression of T_c than Fe for $p < 0.19$ in the presence of the PG. Consistent with this, we also see from Figs. 9(b) and 9(c) that 2% Co and Fe have similar strong pair-breaking effects when there is no PG, but Co and indeed Mn have a stronger effect than Fe in Fig. 9(f), where $p = 0.175$ and there is a small PG.

Overall, our results for Mn, Co, and Fe substitutions show that the details of the d -orbital structure strongly affect the superconducting properties in the underdoped and optimally doped pseudogap region in spite of the fact that they all have approximately the same magnetic moment (although Co is highly anisotropic). Although minimal models such as the single-orbital Hubbard model and the $t - J$ model do account for many unusual properties of high T_c cuprates,^{38,39} understanding the present results seems to require a multi-orbital approach, such as the quantum impurity models reviewed recently.⁴⁰ Our results strongly suggest that Co or Fe substitution will have qualitatively different effects on the local symmetry-breaking seen by STS studies.¹

ACKNOWLEDGMENTS

We gratefully acknowledge financial support for this work from the United Kingdom Engineering and Physical Sciences Research Council and the New Zealand Tertiary Education Commission. We would like to thank C. Hayward of the University of Cambridge Department of Earth Sciences for assistance with EPMA characterization of single crystals, A. Dennis of the Department of Engineering for help with x-ray diffractometry, J. W. Loram and J. L. Tallon for helpful discussions, and also L. Forro of EPF Lausanne and A. Janossy of Budapest University of Technology and Economics for help with electron-spin-resonance experiments.

*Present address: Argonne National Laboratory, 9700 South Cass Avenue, Argonne, Illinois 60439, USA; tbenseman@anl.gov

¹Y. Kohsaka, C. Taylor, P. Wahl, A. Schmidt, Jinhwan Lee, K. Fujita, J. W. Alldredge, K. McElroy, Jinho Lee, H. Eisaki, S. Uchida, D.-H. Lee, and J. C. Davis, *Nature (London)* **454**, 1072 (2008).

²E. W. Hudson, K. M. Lang, V. Madhavan, S. H. Pan, H. Eisaki, S. Uchida, and J. C. Davis, *Nature (London)* **411**, 920 (2002).

³A. Damascelli, Z. Hussain, and Z.-X. Shen, *Rev. Mod. Phys.* **75**, 473 (2003).

⁴H. Alloul, J. Bobroff, M. Gabay, and P. J. Hirschfeld, *Rev. Mod. Phys.* **81**, 45 (2008).

⁵H. V. Kruis, I. Martin, and A. V. Balatsky, *Phys. Rev. B* **64**, 054501 (2001).

⁶A. V. Balatsky, I. V. Vekhter, and J.-X. Zhu, *Rev. Mod. Phys.* **78**, 373 (2006).

⁷D. LeBoeuf, N. Doiron-Leyraud, J. Levallois, R. Daou, J.-B. Bonnemaison, N. E. Hussey, L. Balicas, B. J. Ramshaw, R. Liang, D. A. Bonn, W. N. Hardy, S. Adachi, C. Proust, and L. Taillefer, *Nature (London)* **450**, 533 (2007).

⁸A. Kanigel, M. R. Norman, M. Randeria, U. Chatterjee, S. Souma, A. Kaminski, H. M. Fretwell, S. Rosenkranz, M. Shi, T. Sato, T. Takahashi, Z. Z. Li, H. Raffy, K. Kadowaki, D. Hinks, L. Ozyuzer, and J. C. Campuzano, *Nat. Phys.* **2**, 447 (2006).

⁹B. Vignolle, A. Carrington, R. A. Cooper, M. M. J. French, A. P. Mackenzie, C. Jaudet, D. Vignolles, Cyril Proust, and N. E. Hussey, *Nature (London)* **455**, 952 (2008).

¹⁰J. W. Loram, K. A. Mirza, J. R. Cooper, and J. L. Tallon, *J. Phys. Chem. Solids* **59**, 2091 (1998).

¹¹S. H. Naqib, J. R. Cooper, and J. W. Loram, *Phys. Rev. B* **79**, 104519 (2009).

¹²J. L. Tallon, C. Bernhard, G. V. M. Williams, and J. W. Loram, *Phys. Rev. Lett.* **79**, 5294 (1997).

¹³K. A. Mirza, J. W. Loram, and J. R. Cooper, *Phys. C* **282**, 1411 (1997).

¹⁴R. S. Islam, J. R. Cooper, J. W. Loram, and S. H. Naqib, *Phys. Rev. B* **81**, 054511 (2010).

¹⁵T. Kluge, Y. Koike, A. Fujiwara, M. Kato, T. Noji, and Y. Saito, *Phys. Rev. B* **52**, R727 (1995).

¹⁶Cations and concentrations studied were as follows: $M = \text{Mn}$: $z = 0.0025, 0.005, 0.01, 0.02, 0.04$. $M = \text{Fe}$: $z = 0.005, 0.01, 0.02, 0.04, 0.05, 0.06, 0.08, 0.1$. $M = \text{Co}$: $z = 0.005, 0.01, 0.02, 0.04, 0.06, 0.08, 0.1$. $M = \text{Li}$: $z = 0.005, 0.01, 0.02, 0.03, 0.04, 0.06, 0.08, 0.1$. $M = \text{Al}$: $z = 0.01, 0.02, 0.04$.

¹⁷M. R. Presland, J. L. Tallon, R. G. Buckley, R. S. Liu, and N. E. Flower, *Phys. C* **176**, 95 (1991).

¹⁸T. M. Benseman, Ph.D. thesis, University of Cambridge, 2007.

¹⁹A. Maeda, T. Yabe, S. Takebayashi, M. Hase, and K. Uchinokura, *Phys. Rev. B* **41**, 4112 (1990).

²⁰Y. K. Kuo, C. W. Schneider, M. V. Nevitt, M. J. Skove, and G. X. Tessema, *Phys. Rev. B* **63**, 184515 (2001).

²¹J. Bobroff, W. A. MacFarlane, H. Alloul, P. Mendels, N. Blanchard, G. Collin, and J.-F. Marucco, *Phys. Rev. Lett.* **83**, 4381 (1999).

²²S. D. Obertelli, J. R. Cooper, and J. L. Tallon, *Phys. Rev. B* **46**, 14928 (1992).

²³J. L. Tallon, C. Bernhard, H. Shaked, R. L. Hitterman, and J. D. Jorgensen, *Phys. Rev. B* **51**, 12911 (1995).

²⁴J. R. Cooper and J. W. Loram, *J. Phys. I* **6**, 2237 (1996).

²⁵W. Anukool, S. Barakat, C. Panagopoulos, and J. R. Cooper, *Phys. Rev. B* **80**, 024516 (2009).

²⁶M. Babaei pour and D. K. Ross, *Phys. C* **425**, 130 (2005).

²⁷J. W. Loram (private communication).

²⁸T. M. Benseman, J. R. Cooper, and G. Balakrishnan, *Phys. C* **468**, 81 (2007).

²⁹T. Watanabe, T. Fujii, and A. Matsuda, *Phys. Rev. Lett.* **84**, 5848 (2000).

³⁰J. R. Cooper *et al.* (unpublished).

³¹C. Kittel, *Introduction to Solid State Physics*, 6th ed. (Wiley, New York, 1986), p. 402.

³²W. Anukool, Ph.D. thesis, University of Cambridge, 2003.

³³Z. Hao and J. R. Clem, *Phys. Rev. Lett.* **67**, 2371 (1991).

³⁴G. Triscone, A. F. Khoder, C. Opagiste, J.-Y. Genoud, T. Graf, E. Janod, T. Tsukamoto, M. Couach, A. Junod, and J. Muller, *Phys. C* **224**, 263 (1994).

³⁵L. N. Bulaevskii, M. Ledvij, and V. G. Kogan, *Phys. Rev. Lett.* **68**, 3773 (1992).

³⁶A. Junod, J.-Y. Genoud, G. Triscone, and T. Schneider, *Phys. C* **294**, 115 (1998).

³⁷J. R. Cooper, in *High Temperature Superconductivity: Proceedings of LT-19 Satellite Conference, Cambridge, 13-15 August 1990*, edited by J. Evetts (A. Hilger, Bristol, 1991), pp. S181–S183.

³⁸J. Jaklič and P. Prelovšek, *Adv. Phys.* **49**, 1 (2000).

³⁹E. Plekhanov, F. Becca, and S. Sorella, *Phys. Rev. B* **71**, 064511 (2005).

⁴⁰E. Gull, A. J. Millis, A. I. Lichtenstein, A. N. Rubtsov, M. Troyer, and P. Werner, *Rev. Mod. Phys.* **83**, 349 (2011).